A Note on the Classical Buckling Load of Circular Cylindrical Shells under Axial Compression

R. C. TENNYSON*
Institute of Aerophysics, University of Toronto

EXPERIMENTS made to verify the theoretical results of the classical linear theory have shown that, in contrast to experience gained with other thin structural elements —e.g., plates and bars—the buckling of thin cylinders under axial compression shows large differences from the predicted values. Buckling loads are on the average only 20 to 30 percent of the classical values and exhibit unusually large scatter.[1] A comparison between experiments and the classical theory is summarized in Ref. 2.

However, recent experiments by the author on a thin-walled circular cylinder under axial compression with no excess internal pressure have repeatedly yielded results very close to the classical buckling load.

Test cylinders were made from a liquid photoelastic plastic spun-cast in an acrylic tube. The tube was attached to a lathe which produces sufficient rotational energy to spin-cast the polymer inside the shell form. To insure an absolutely circular cross section, a Hysol plastic shell was first cast in the acrylic tube. High rotational velocities of the order of 800 rpm were necessary in order to distribute the liquid evenly in the form and to yield a circular shape. Centrifugal force drives out the air bubbles which are trapped in the liquid and produces a smooth imperfection-free shell wall. Careful alignment of the form can result in a thickness variation as low as ± 6 percent.

At present, only one photoelastic model has been tested. However, the buckling load of the model was repeatable as many as 19 times, and each value was within 10 percent of the calculated classical load. Buckling of the shell was completely elastic and was taken as the maximum load sustained in the testing machine. Fig. 1 illustrates a typical test run on the model using a circular reflection polariscope to determine the linear strain distribution up to buckling. Standard photoelastic techniques were employed. The striped pattern visible on the cylinder in Fig. 1 occurs because of two reflective surfaces cast at different thicknesses in the shell's wall.

During a particular test run, a high-speed Fastax camera was used to photograph the buckling mechanism at a rate of 1,000 pps. (Fig. 2).

From Fig. 2 it can be estimated that the buckling process occurs in approximately 0.006 sec. What is of more immediate interest is the fact that initially two smaller buckles formed and rapidly converged into one larger "diamond" or elliptically shaped buckle. For the particular cylinder geometry, theory[3] indicates that initially 12 buckles should form which, at the end of the buckling process, should emerge as six larger buckles. Six buckles did form at the end of the buckling process and were located circumferentially around the cylinder. From Fig. 2 one may conclude that 12 buckles did exist at the start of buckling. It is intended that a faster framing rate be used in an attempt to catch a square-wave pattern to compare with the classically predicted wave shape.

Equilibrium states of the shell have been discovered in close agreement with the experimentally observed ones, both in applied load and wave pattern, which involve a much lower applied load than that predicted by the classical theory. This has led some to conclude that the unbuckled shell will suddenly jump to those equilibrium positions during the loading process without ever reaching the classical value—e.g., the imperfection theory[2] and Tsien's energy criterion.[1]

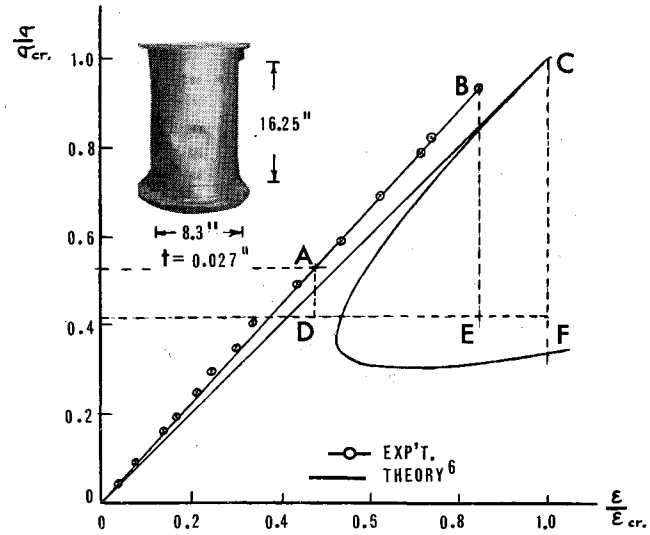

Fig. 1 Critical stress ratio vs critical strain ratio for a circular cylindrical shell under end compression. (A = axial compressive stress, σ_{cr} = critical compressive stress, ϵ = axial compressive strain, ϵ_{cr} = critical compressive strain, t = shell-wall thickness, pps = pictures per sec). Critical buckling loads (A = external radial load, B = no external disturbance, C = classical buckling load). Post-buckling loads (D = with external load, E = no external disturbance, F = theoretical value)

Since the cylinder tested was relatively imperfection-free, then according to Tsien's criterion, under average laboratory conditions, disturbances of sufficient magnitude will always exist so that buckling of a cylinder must occur at a load 40–60 percent of the classical value. However, with the test specimen used, Tsien's lower buckling load was achieved only when an external lateral load was deliberately superimposed on the shell walls (Fig. 1). The shell, when left to buckle on its own accord, reached within 10 percent of the predicted

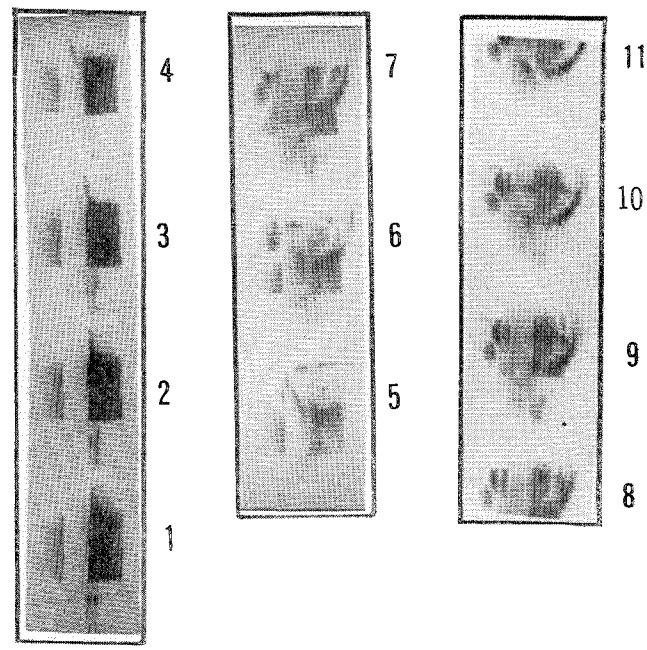

Fig. 2 The buckling process as viewed through a circular reflection polariscope. Frame 3, start of the buckling process, frame 6, emergence of two distinct small buckles, frame 8, final buckle form as visible on cylinder (Fig. 1)

Received by IAS August 23, 1962.
* Research Assistant.

classical value. Therefore, it is tentatively concluded that when tests are performed on isotropic elastic cylinders sufficiently free of imperfections, axially loaded in a rigid test machine, the classical value can be attained and a lower buckling load is not always inevitable.

References

[1] Thielmann, W. F., "Buckling of thin cylindrical shells," *Aero. & Astro. Proc. of the Durand Cent. Conf.* (Pergamon Press, London, 1960), Vol. 9, Div. IX, pp. 76–119.

[2] Donnell, L. H. and Wan, C. C., "Effect of imperfections on buckling of thin cylinders and columns under axial compression," J. Appl. Mech. **17**, 73 (1950).

[3] von Kármán, T. and Tsien, H. S., "The buckling of thin cylindrical shells under axial compression," J. Aeron. Sci. **8** (Aug. 1941).

The Effect of a Cavity on Panel Vibration

E. H. Dowell* and H. M. Voss*
The Boeing Company, Seattle, Wash.

THE dynamic behavior of plates has recently acquired new interest in relation to their aeroelastic stability and excitation by noise. A prerequisite for studying such phenomena is the ability to predict the so-called natural modes and frequencies of the plate. One of the factors which may significantly alter the idealized model of a plate vibrating "in vacuo" is an underlying cavity. Here we present the results of an analysis of the system shown in Fig. 1. The model consists of a rectangular box of which one side is a vibrating plate.

We will assume the amplitude of motion is sufficiently small so that the linearized form of the governing flow equations and equations of elasticity may be employed. As is shown in numerous references, the flow field of compressible, inviscid fluid may be described by a velocity potential which satisfies the acoustic equation,

$$\frac{\partial^2\varphi}{\partial x^2} + \frac{\partial^2\varphi}{\partial y^2} + \frac{\partial^2\varphi}{\partial z^2} = \frac{1}{a^2}\frac{\partial^2\varphi}{\partial t^2} \tag{1}$$

where φ is the velocity potential. The appropriate boundary conditions for our problem are

$$\frac{\partial\varphi}{\partial n} = 0 \qquad \begin{cases} x = 0,l \\ y = 0,b \\ z = d \end{cases} \tag{2}$$

and

$$\partial\varphi/\partial z = \partial W/\partial t \qquad z = 0 \tag{3}$$

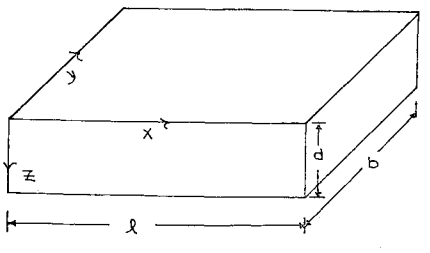

Fig. 1

Received by IAS August 27, 1962. This work was carried out under AF 33(616)-8081 sponsored by the Aeronautical Systems Division, Air Force Systems Command, Wright Patterson Air Force Base, Ohio.

* Structures Department.

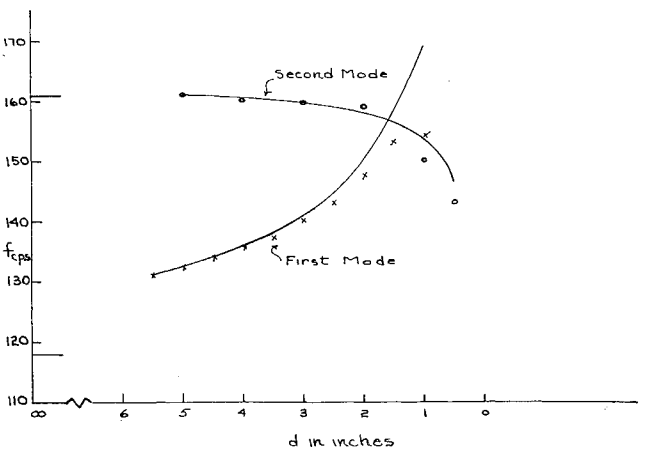

Fig. 2 Panel frequency vs cavity depth

where W is the plate deflection. We further assume a cosine-series expansion of the deflection,

$$W = \sum_m \sum_n \left[w_{mn} \cos\frac{m\pi x}{l} \cos\frac{n\pi y}{b} e^{i\omega t} \right] \tag{4}$$

Solving the system of Eqs. (1), (2), (3), using Eq. (4) gives

$$\varphi = i\omega e^{i\omega t} \sum_m \sum_n \left[\frac{w_{mn}}{v_{mn}} (\sinh v_{mn}z - \coth v_{mn}d \cosh v_{mn}z) \right] \cos\frac{m\pi x}{l} \cos\frac{n\pi y}{b} \tag{5}$$

where

$$v_{mn}^2 = \pi^2[(m/l)^2 + (n/b)^2] - (\omega/a)^2 \tag{6}$$

The pressure on the panel may be computed from the linearized form of Bernoulli's equation,

$$P = \rho\omega^2\epsilon^{i\omega t} \sum_m \sum_n w_{mn} \frac{\coth v_{mn}d}{v_{mn}} \cos\frac{m\pi x}{l} \cos\frac{n\pi y}{b} \tag{7}$$

It may be noted that the nature of the pressure loading is dependent on the magnitude and sign of v_{mn}^2 and hence on the relative dimensions of panel and cavity. The quantity $a^2v_{mn}^2$ represents the difference in the squares of the frequencies of the natural cavity modes and the panel modes, and the pressure loading will be a maximum when this quantity is a minimum. However, for most panels, the frequency spectrum is such that all panel modes of interest lie between the cavity normal mode ($m = n = 0$) and the transverse mode ($m, n = 1, 0$). For practical panels and small cavity depths, it may be concluded that the principal effect on the

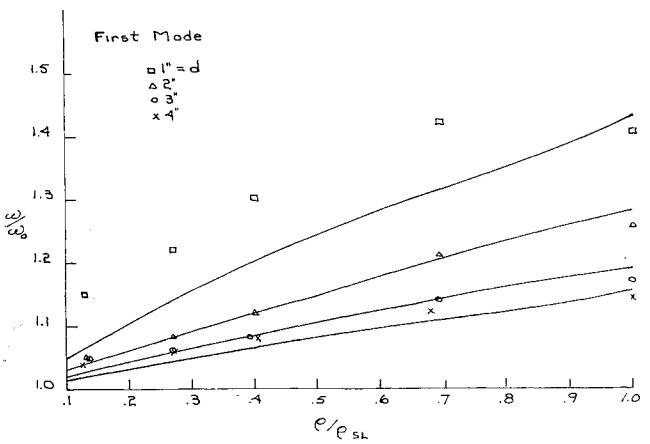

Fig. 3 Panel frequency vs cavity density